

# Epimedin C: A promising neuroprotective agent that can participate in mediating the JNK/Nrf2/HO-1 signaling pathway to prevent neurodegenerative diseases

CHAO CONG<sup>\*</sup>, XUAN-LING LI<sup>\*</sup>, GUANG-YAO LIN and LIAN-WEI XU

Department of Gynecology, Longhua Hospital, Shanghai University of Traditional Chinese Medicine, Shanghai 200032, P.R. China

Received May 21, 2025; Accepted September 23, 2025

DOI: 10.3892/etm.2025.12998

**Abstract.** *Epimedium* can be used to treat neurodegenerative diseases. Flavonol glycosides are the major bioactive compounds within *Epimedium* extract, including icariin and Epimedin C, which is found at the highest concentration among all flavonol glycosides. The present study aimed to explore the potential pharmacological mechanisms by which Epimedin C prevents neurodegenerative diseases. The present study first identified the active ingredients in *Epimedium* by performing ultra-high performance liquid chromatography-quadrupole-Exactive Orbitrap high resolution mass spectrometry (UHPLC-Q-Exactive Orbitrap HRMS). Subsequently, its potential mechanism in preventing neurodegenerative diseases was explored by combining the identification results with network pharmacological analysis (using Alzheimer's disease as an example). Subsequently, the optimal concentration of Epimedin C for the intervention of PC12 cells was screened using Cell Counting Kit-8 (CCK-8). PC12 cells were divided into the following groups: Normal control, H<sub>2</sub>O<sub>2</sub> (150 μM for 4 h), or 24 h pretreatment with either 17β-estradiol (1 nM) or Epimedin C (1, 5 and 10 μM) followed by exposure to H<sub>2</sub>O<sub>2</sub> (150 μM for 4 h). Lactate dehydrogenase was measured to detect the cytotoxicity of each group under different intervention methods, and malondialdehyde and reactive oxygen species assay kits were employed to detect the oxidative stress (OS) of each group of cells. Subsequently, the apoptosis levels of each group were evaluated by flow cytometry and TUNEL staining. Transmission electron microscopy and JC-1 were adopted to evaluate the mitochondrial function of cells. Subsequently, according to network

pharmacological analysis, western blotting was performed to detect the protein levels of JNK, phosphorylated (p)-JNK, nuclear factor erythroid 2-related factor 2 (Nrf2), heme oxygenase-1 (HO-1), Bcl-2 and Bax in cells. Finally, to further verify whether Epimedin C mediates the JNK pathway, the JNK agonist anisomycin was added to the PC12 cells after H<sub>2</sub>O<sub>2</sub> intervention and after H<sub>2</sub>O<sub>2</sub> combined with Epimedin C intervention. The differences in protein levels in PC12 cells under different intervention methods were then compared. The CCK-8 results showed that cells treated with Epimedin C at concentrations of 1, 5 and 10 μM had improved cell survival rates compared with other concentrations. When compared with the control group, the H<sub>2</sub>O<sub>2</sub>-induced group displayed severe OS damage and a significantly increased incidence of apoptosis. By contrast, after intervention with Epimedin C, the OS damage in PC12 cells was markedly inhibited and mitochondrial apoptosis was evidently decreased. Among the concentrations, 10 μM Epimedin C had a more notable effect. Through UHPLC-Q-Exactive Orbitrap HRMS plus network pharmacological analysis, 108 shared targets (with Alzheimer's disease) were enriched, and the top 20 core genes included BCL2, APP and JUN. The results of Gene Ontology and Kyoto Encyclopedia of Genes and Genomes analyses revealed that the common targets were closely related to apoptosis. The results of the western blot double validation experiment also confirmed that the JNK pathway was significantly activated in PC12 cells exposed to H<sub>2</sub>O<sub>2</sub>, and that Epimedin C can inhibit JNK phosphorylation. Notably, western blotting results showed that compared with in the H<sub>2</sub>O<sub>2</sub> group, after intervention with Epimedin C, p-JNK was significantly downregulated, Nrf2 and HO-1 were significantly upregulated, BAX was significantly downregulated and Bcl-2 was upregulated. In conclusion Epimedin C may improve OS in PC12 cells, exert neuroprotective effects and reduce apoptosis by inhibiting JNK phosphorylation and activating Nrf2/HO-1. Epimedin C may thus be considered a potential candidate neuroprotective agent for preventing neurodegenerative diseases.

---

*Correspondence to:* Professor Lian-Wei Xu, Department of Gynecology, Longhua Hospital, Shanghai University of Traditional Chinese Medicine, 725 Wanping South Road, Xuhui, Shanghai 200032, P.R. China  
E-mail: xu\_lianwei2800@shutcm.edu.cn

<sup>\*</sup>Contributed equally

**Key words:** Epimedin C, neuroprotective agent, JNK/Nrf2/HO-1, oxidative damage, apoptosis, neurodegenerative diseases

## Introduction

Neurodegenerative diseases can result in the gradual loss of neuronal function or structure in the central nervous system (CNS), and include Alzheimer's disease (AD) and motor neuron disease (1). A pathological feature of these diseases is

the abnormal deposition of proteins, such as amyloid  $\beta$  ( $A\beta$ ) and tau, in the brain and spinal cord (2). Various neurodegenerative diseases display specific differences, but they all exhibit common clinical features; namely, the progressive loss of cognitive function, motor coordination deficits and various symptoms resulting from the loss of specific neuronal groups (3). Neurodegenerative diseases affect millions of individuals worldwide (4). The prevalence and mortality rates have also shown a growing trend over time, and these diseases are considered one of the main threats to personal and social well-being (4). Oxidative stress (OS) serves an important role in the pathogenesis of neurodegenerative diseases (5,6). The CNS is particularly susceptible to OS because of its high oxygen utilization rate and large polyunsaturated fatty acid contents (7). Therefore, the antioxidant inhibition of OS is considered a therapeutic strategy for neurodegenerative diseases due to its ability to neutralize reactive oxygen species (ROS), which is of therapeutic relevance for reducing the progression of OS.

Neurodegenerative diseases have become one of the largest health problems worldwide, and there is still a shortage of appropriate treatment methods (8). Traditional Chinese medicine (TCM) displays multi-component and multi-target characteristics, providing a promising method for preventing neurodegenerative diseases (9). The compounds and extracts derived from TCM, such as evodiamine from *Tetradium ruticarpum* and ginsenoside compound K from *Panax ginseng*, have received widespread attention due to their possible applications as therapeutic agents for AD and Parkinson's disease (10). In clinical practice, TCM has been extensively utilized for treating age-related conditions, including memory loss and cognitive decline (11,12). Furthermore, bioactive compounds in plants, such as genipin from *Gardenia jasminoides* fruit extract, had been proven to possess the ability to prevent and stop the progression of AD and Parkinson's disease (8). They can regulate crosstalk between pathways through multiple targets, thus improving chronic inflammatory interactions and inhibiting OS damage (13). The leaves, stems and rhizomes of *Epimedium*, also known as barrenwort, can be used as therapeutic drugs (14). Pharmacological studies have shown that *Epimedium* can markedly regulate and improve the human immune system, and the chemicals in *Epimedium* have great potential as plant drugs for guarding against and treating chronic diseases such as AD (15,16). Notably, >260 compounds have been extracted from *Epimedium* (16), and research has suggested that the compound icariin possesses strong neuroprotective properties and has the potential as a drug for preventing neurological disorders such as AD (17). However, the main bioactive chemicals and their specific mechanisms that exert antioxidative, anti-aging and neuroprotective effects in *Epimedium* still require further exploration.

The median effect concentration value of Wushanicaritin in PC12 cells is 3.87  $\mu$ M, making it a promising neuroprotective agent (16). In addition, Wushanicaritin has been shown to maintain mitochondrial activity and the enzymatic antioxidant defense system, demonstrating marked intercellular antioxidant and neuroprotective effects (16). Epimedin C was used as the indicator component in the quality control for assessing the quality of Wushan *Epimedium* in the Chinese Pharmacopoeia (2020 edition) (18). A previous study

confirmed that total flavonoids of *Epimedium* can prevent dopaminergic neuron death and cellular neurotoxicity *in vivo* and *in vitro*, exerting neuroprotective effects (19). Epimedin C is a triterpenoid component extracted from the water extract of *Epimedium*, containing high levels of flavonol glycosides (20). The chemical structure of Epimedin C is similar to that of icariin, indicating that they may have similar pharmacological effects (21). Moreover, Epimedin C has been reported to exert anti-inflammatory properties (21), and to have potential therapeutic efficacy in angiogenesis, antioxidant damage and the inhibition of apoptosis (22). However, it is currently unclear whether Epimedin C can reduce neuronal cell apoptosis by inhibiting oxidative damage, thereby preventing and/or treating neurodegenerative diseases such as AD.

The PC12 rat adrenal pheochromocytoma cell line is often adopted as a model neuron-like cell line and applied to study neurodegenerative diseases (23). Exogenous  $H_2O_2$  can trigger OS damage and cause apoptosis of PC12 cells (24). Our previous research indicated that Tiaogeng Decoction (TGD) may be a potential therapeutic agent for the treatment of neurodegenerative diseases, as it is involved in mediating the nuclear factor erythroid 2-related factor 2 (Nrf2) and JNK pathways (25). Notably, TGD comprises 10 TCMs, including *Epimedium*. A core component of neuronal response to ROS is the activation of JNK (26); JNK belongs to the mitogen-activated protein kinase (MAPK) family, and JNK phosphorylation is associated with diverse apoptotic transcription factors (27). Nrf2 participates in maintaining cellular redox homeostasis and regulating the inflammatory response of the body, and Nrf2 activation has a cellular protective effect on neurodegenerative diseases (28). Heme oxygenase-1 (HO-1) serves as a protective protein during the OS response (29). Nrf2/HO-1 pathway activation accelerates the upregulation of antioxidant and cell protective genes, thereby reducing OS and inflammatory damage (30). Ultra-high performance liquid chromatography-quadrupole-Exactive Orbitrap high resolution mass spectrometry (UHPLC-Q-Exactive Orbitrap HRMS) can be utilized to rapidly identify complex compound mixtures in plants (31). The present study aimed to assess the active ingredients of *Epimedium* using UHPLC-Q-Exactive Orbitrap HRMS. In addition to mass spectrometry results, network pharmacological analysis was performed to explore whether Epimedin C mediated the JNK/Nrf2/HO-1 pathway, and prevented the  $H_2O_2$ -related OS damage and apoptosis of PC12 cells. Moreover, the present study aimed to clarify the possible effect of Epimedin C on managing neurodegenerative diseases.

## Materials and methods

*Identification of chemical components in Epimedium by UHPLC-Q-Exactive Orbitrap HRMS.* In our previous research, UHPLC-Q-Exactive Orbitrap HRMS analysis was conducted on TGD (11). By comparing and analyzing the chemical composition of each herb detected in the viscera and serum of rats after oral administration of TGD, the effective chemical components of each TCM that worked in the formula were explored. *Epimedium* is an important component of TGD. A total of 250 mg *Epimedium* sample (Sichuan Neo-Green Pharmaceutical Technology

Development Co., Ltd.) was taken and placed in a 2ml centrifuge tube. Thereafter, 20% methanol (4 ml) was added for centrifugation (4°C, 10,000 x g, 15 min). Subsequently, 200 µl supernatant was taken as the experimental sample. Chromatographic separation was implemented through a Waters ACQUITY UPLC BEH C18 column (2.1x100 mm, 1.7 µm; Waters Corporation) at a column temperature of 40°C. The mobile phase included two solvents; mobile phase A consisted of methanol whereas mobile phase B comprised a 0.1% formic acid aqueous solution. Elution was completed according to the following schedule: 4% A from 0 to 4.0 min, 4-12% A at 4.0-10.0 min, 12-70% A at 10.0-30.0 min, 70-95% A at 30.0-35.0 min, 95% A at 35.0-38.0 min, and 4% A at 42.0-45.0 min. The flow rate was 0.3 ml/min and the injection volume was 2 µl. The resolution was 70,000 full width at half maximum and the cumulative time was 300 msec. Data collection and analysis of the results of UHPLC-Q-Exactive Orbitrap HRMS analysis (Thermo Fisher Scientific, Inc.) were performed using Xcalibur 4.1 software (Thermo Fisher Scientific, Inc.).

*Network pharmacological analysis: Target prediction of Epimedium for improving AD.* Drug targets were retrieved using the key word 'Epimedium' in the TCM systems pharmacology (TCMSP) (<https://www.91tcmsp.com/>), SwissTarget (<http://swisstargetprediction.ch/>), PharmMapper (<http://lilab-ecust.cn/pharmmapper/>) and HERB databases (<http://herb.ac.cn/>), utilizing the criteria oral bioavailability ≥30% and drug similarity ≥0.18. Subsequently, with 'Alzheimer's disease' being used as the key word, drug targets were searched in the GeneCards (<https://www.genecards.org/>), DisGeNet (<https://disgenet.com>) and Online Mendelian Inheritance In Man (OMIM) databases (<https://www.omim.org/>), and Venn diagrams (<http://bioinformatics.psb.ugent.be/webtools/Venn/>) were used to screen and generate overlapping targets between diseases and drugs. The 'drug disease target' was visualized with Cytoscape 3.8.2 (<https://cytoscape.org/download.html>), while common targets of drugs were imported in STRING database (<https://string-db.org/>) for protein-protein interaction (PPI) analysis. In the PPI network, proteins were denoted by nodes, whereas protein interactions were signified by edges. Nodes of various colors and sizes represented diverse degree values, and larger nodes and darker red colors declared greater degree values and more important targets. Gene Ontology (GO) and Kyoto Encyclopedia of Genes and Genomes (KEGG) enrichment analyses were performed on the top 20 core targets in Metascape database (<https://metascape.org/gp/index.html>). Subsequently, the exported clustering network was sorted in accordance with the P-value using R 4.1.2 (<https://www.r-project.org/>) and a bubble chart was generated.

*Chemicals and reagents.* Epimedin C was supplied by Chengdu Biopurify Phytochemicals Ltd. (CAS no. 110642-44-9), and its purity was detected by HPLC-Diode Array Detection to be 95-99%. In addition, 17β-estradiol (17β-E<sub>2</sub>) was provided by Sigma-Aldrich; Merck KGaA (cat. no. E2758). All samples were stored in the laboratory at 4°C for future use.

*Modeling and intervention.* PC12 cells were obtained from The Cell Bank of Type Culture Collection of The Chinese Academy of Sciences and were cultured in the Dulbecco's Modified Eagle medium (cat. no. C11995500BT; Gibco; Thermo Fisher Scientific Inc.) with 10% FBS (cat. no. 10099-141C; Gibco; Thermo Fisher Scientific Inc.) at 37°C and 5% CO<sub>2</sub>. The compound 17β-E<sub>2</sub> can be produced in the brain and it participates in regulating the reproductive axis (32). In addition, it can act on synaptic plasticity, and improve neural pathways and neurodegenerative diseases (32-34). Therefore, the present study used 17β-E<sub>2</sub> in the positive control group. PC12 cells were classified into the normal control, H<sub>2</sub>O<sub>2</sub> model, 17β-E<sub>2</sub> and Epimedin C (1, 5 and 10 µM) groups. A concentration of 150 µM H<sub>2</sub>O<sub>2</sub> (25) (cat. no. 7722-84-1; Sigma-Aldrich; Merck KGaA) was applied for 4 h at 37°C and 5% CO<sub>2</sub> to induce OS within PC12 cells in the model and treatment groups. A total of 24 h before H<sub>2</sub>O<sub>2</sub> treatment, Epimedin C (1, 5 and 10 µM) was introduced into the TCM groups, whereas 17β-E<sub>2</sub> (1 nM) was added into the positive control group for 24 h at 37°C and 5% CO<sub>2</sub>. To determine whether the JNK pathway affected Epimedin C-induced Nrf2 activation, PC12 cells from the model and treatment groups were also treated with the JNK agonist anisomycin (5 µM; cat. no. S7409; Selleck Chemicals). Following 4 h of H<sub>2</sub>O<sub>2</sub> treatment, the culture medium was removed, and the cells were further incubated with anisomycin for 24 h at 37°C and 5% CO<sub>2</sub>.

*Cell viability and toxicity assays.* The cultured cells were digested, centrifuge at 1,200 x g for 5 min at 25°C and counted. Subsequently, cells (2x10<sup>4</sup>/well) were seeded into a 96-well plate and were cultured for 12 h under 37°C, 5% CO<sub>2</sub> and 90% humidity conditions. The cells were then treated with different concentrations of Epimedin C (0-160 µM) for 24 h at 37°C and 5% CO<sub>2</sub>. Subsequently, cell viability was assessed according to the instructions of the Cell Counting Kit-8 (cat. no. GK3607; Gen-View Scientific Inc.) and the optimal drug administration concentration was screened. In addition, according to the manufacturer's instructions, a lactate dehydrogenase (LDH) detection kit (cat. no. C0016; Beyotime Institute of Biotechnology) was used to assess the cytotoxicity of Epimedin C at different concentrations (0-160 µM) to evaluate their safety. Six replicates were set for each sample and the absorbance was measured at 450 nm for the CCK-8 assay and at 490 nm for the LDH assay using a microplate reader (BioTek; Agilent Technologies, Inc.).

*ROS and malondialdehyde (MDA) level measurements.* The ROS assay kit (cat. no. S0033; Beyotime Institute of Biotechnology) was adopted to detect cellular ROS levels. PBS was introduced to dilute DCFH-DA to 10 µmol/l. After removing the culture medium, the diluted DCFH-DA at 10 µM was added and the cells were incubated for 20 min at 37°C. The cells were then rinsed three times with PBS to thoroughly remove the DCFH-DA that had not entered the cells. A microplate reader (BioTek; Agilent Technologies, Inc.) was adopted for testing ROS levels. The fluorescence was measured at an excitation wavelength of 485 nm and an emission wavelength of 525 nm.

The lipid peroxidation level in PC12 cells was evaluated using the MDA assay kit (cat. no. S0131S; Beyotime Institute

of Biotechnology). PC12 cells ( $1 \times 10^4$ /well) were collected and lysed using RIPA lysis buffer (cat. no. P0013K; Beyotime Institute of Biotechnology). The cell lysate was then centrifuged at  $12,000 \times g$  for 5 min at  $4^\circ\text{C}$  to remove insoluble debris. Finally, the absorbance of the resulting supernatant was measured at 532 nm using a microplate reader. The MDA concentration in the samples was calculated based on a standard curve prepared concurrently.

**Transmission electron microscopy (TEM).** The PC12 cells were scraped and digested into a cell suspension, and were immediately fixed with 2.5% glutaraldehyde in 0.1 M phosphate buffer (pH 7.4) for 24 h at  $4^\circ\text{C}$ . Following primary fixation, the cells were post-fixed in 1%  $\text{OsO}_4$  tetroxide for 2 h at  $4^\circ\text{C}$ , then dehydrated through a graded series of ethanol (50, 70, 90 and 100%). The dehydrated cells were embedded in epoxy resin. Ultrathin sections were cut using an ultramicrotome at a thickness of 70-90 nm and collected on copper grids. The sections were then stained with 1% uranyl acetate at room temperature for 10 min, and the samples were observed using a Talos L120C transmission electron microscope (Thermo Fisher Scientific, Inc.) operated at an accelerating voltage of 80-120 kV. Digital images were acquired for analysis.

**TUNEL analysis.** After intervention with different groups of drugs, PC12 cells were immersed in 4% paraformaldehyde for 30 min at  $4^\circ\text{C}$ , after which the cells were rinsed three times with PBS and permeabilized using 0.1% Triton X-100 for 3 min at  $25^\circ\text{C}$ . Subsequently, the TUNEL reaction solution (cat. no. C1170S; Beyotime Institute of Biotechnology) was added to the cells and incubated for 1 h in the dark at  $37^\circ\text{C}$ . The cells were then rinsed with PBS and later subjected to nuclear counterstaining with DAPI (cat. no. C1006; Beyotime Institute of Biotechnology) at room temperature for 5 min. The number of TUNEL-positive cells from five random regions in three individual samples was quantified using a fluorescence microscope (Ti-E; Nikon Corporation), and TUNEL-positive cell rate (%) was calculated as: TUNEL-positive cell area/total cell area  $\times 100$ .

**Flow cytometry.** Flow cytometry was applied for the quantitative analysis of apoptosis and mitochondrial membrane potential (MMP) in PC12 cells, using the CytExpert software (version 2.5; Beckman Coulter, Inc.) for analysis. The Annexin V-FITC/PI cell apoptosis detection kit (cat. no. 556547; BD Biosciences) was utilized for detecting cell apoptosis. Briefly, cells ( $2 \times 10^5$ /well) were harvested and resuspended in  $400 \mu\text{l}$  binding buffer. Thereafter, Annexin V-FITC and PI ( $5 \mu\text{l}$  each) were added and mixed, and the cells were incubated in the dark for 15 min at room temperature. Afterwards, flow cytometry (CytoFLEX SRT; Beckman Coulter Inc.) was used to analyze early and late apoptotic cell proportion.

The level of MMP can reflect the status of apoptosis. Briefly, the cells ( $2 \times 10^5$ /well) were cultured in a 6-well plate and rinsed once with PBS. Subsequently, 1 ml JC-1 (cat. no. C2006; Beyotime Institute of Biotechnology) staining solution was introduced, mixed sufficiently with the media and incubated at  $37^\circ\text{C}$  in an incubator for 20 min. Afterwards, the supernatant was discarded, and the sample was rinsed twice with JC-1

staining buffer (1X). An Altra flow cytometer (CytoFLEX SRT; Beckman Coulter Inc.) was used to verify the changes in MMP in each group of cells. The JC-1 aggregates (healthy mitochondria) were detected in the PE channel (575 nm emission), while the JC-1 monomers (depolarized mitochondria) were detected in the FITC channel (530 nm emission). The ratio of the geometric mean fluorescence intensity (PE/FITC) was calculated to quantify the MMP.

**Western blotting (WB).** After treatment, PC12 cells were subjected to lysis with RIPA buffer that contained 1% PMSF (cat. no. ST506; Beyotime Institute of Biotechnology). The BCA protein detection kit (cat. no. P0011; Beyotime Institute of Biotechnology) was used to measure protein concentration. Subsequently, PBS and 4X loading buffer were added according to protein concentration, mixed evenly and boiled at  $95^\circ\text{C}$  for 10 min. Proteins ( $20 \mu\text{g}/\text{lane}$ ) were separated by SDS-PAGE on 10% gels and were then transferred to polyvinylidene fluoride membranes (cat. no. ISEQ00010; Merck KGaA). After blocking for 1 h at room temperature in 5% BSA (Beyotime Institute of Biotechnology), the membranes were subjected to primary antibody incubation overnight at  $4^\circ\text{C}$  using antibodies against: GAPDH (1:1,000; cat. no. 5174; CST Biological Reagents Co., Ltd.), JNK (1:1,000; cat. no. 9252; CST Biological Reagents Co., Ltd.), phosphorylated (p)-JNK (1:1,000; cat. no. 4668; CST Biological Reagents Co., Ltd.), HO-1 (1:1,000; cat. no. 43966; CST Biological Reagents Co., Ltd.), Bcl-2 (1:1,000; cat. no. 2870; CST Biological Reagents Co., Ltd.), Bax (1:1,000; cat. no. 14796; CST Biological Reagents Co., Ltd) and Nrf2 (1:500; cat. no. ab137550; Abcam). The next day, the membranes were washed six times with TBS-0.01% Tween and were incubated with a HRP-conjugated Goat Anti-Rabbit IgG (H+L) secondary antibody (1:10,000; cat. no. 33101ES60; Shanghai Yeasen Biotechnology Co., Ltd) at room temperature for 1 h. After incubation, the membranes were washed six times with TBST. Subsequently, the membranes were visualized using Omni-ECL (Epizyme; Ipsen Pharma). The gel imaging system (Chemiscope6300; Clinx Science Instruments Co., Ltd.) was used for imaging and semi-quantification was performed using ImageJ (version 1.6.0; National Institutes of Health).

**Statistical analysis.** Data are presented as the mean  $\pm$  SD. Unpaired Student's t-tests were used for pairwise comparisons between two groups. For comparisons across more than two groups, the homogeneity of variances was first assessed using Levene's test. Following a significant Levene's test ( $P < 0.05$ ) which indicated heterogeneity of variances, a Welch's ANOVA was conducted in place of the standard one-way ANOVA. Post hoc comparisons against the control or  $\text{H}_2\text{O}_2$  group were then performed using Dunnett's T3 test to account for the unequal variances. In cases where Levene's test was not significant ( $P > 0.05$ ), indicating homogenous variances, a standard one-way ANOVA was performed, followed by Bonferroni's post hoc test for all comparisons against the control or  $\text{H}_2\text{O}_2$  group. GraphPad Prism version 9.3 (Dotmatics) was employed for data analysis.  $P < 0.05$  was considered to indicate a statistically significant difference.

Table I. Identification of active ingredients in *Epimedium* that can enter the bloodstream.

Number	RT, min	Precursor ion	Measured mass, Da	Calculated mass, Da	Error, ppm	Formula	Identification
1	12.24	(M-H)-	337.09348	337.09179	1.793	C <sub>16</sub> H <sub>18</sub> O <sub>8</sub>	3-O-p-coumaroylquinic acid
2	16.09	(M-H)-	479.08377	479.08201	0.987	C <sub>21</sub> H <sub>20</sub> O <sub>13</sub>	Isoyangmei bark glycoside
3	16.45	(M-H)-	447.09393	447.09218	1.235	C <sub>21</sub> H <sub>20</sub> O <sub>11</sub>	Trifolin
4	18.38	(M-H)-	464.09064	463.08710	6.321	C <sub>21</sub> H <sub>20</sub> O <sub>12</sub>	Hyperin
5	21.34	(M-H)-	576.17704	577.15518	0.163	C <sub>27</sub> H <sub>30</sub> O <sub>14</sub>	Kaempferitrin
6	22.94	(M-H)-	465.23335	465.21190	-1.173	C <sub>24</sub> H <sub>34</sub> O <sub>9</sub>	(4-(β-D-glucopyranosyloxy)-2,6-bis(3-methyl-2-buten-1-yl)phenyl)(hydroxy)acetic acid
7	23.39	(M-H)-	677.2199	677.20761	2.394	C <sub>32</sub> H <sub>38</sub> O <sub>16</sub>	Hexandraside E
8	24.03	(M-H)-	678.21332	678.20761	0.032	C <sub>32</sub> H <sub>38</sub> O <sub>16</sub>	Epimedium B
9	25.6	(M-H)-	661.21472	661.21269	1.960	C <sub>32</sub> H <sub>38</sub> O <sub>15</sub>	Epimedium A
10	25.95	(M-H)-	807.27338	807.27060	0.166	C <sub>38</sub> H <sub>48</sub> O <sub>19</sub>	Epimedin B
11	26.06	(M-H)-	691.22565	691.22326	2.223	C <sub>33</sub> H <sub>40</sub> O <sub>16</sub>	Anhydroicaritin-3,7-di-O-glucoside
12	28.95	(M-H)-	515.15625	515.15478	0.237	C <sub>26</sub> H <sub>28</sub> O <sub>11</sub>	Epimedin C
13	29.55	(M-H)-	675.23077	675.22834	2.342	C <sub>33</sub> H <sub>40</sub> O <sub>15</sub>	Baohuoside VII
14	29.94	(M-H)-	645.22003	645.21778	2.636	C <sub>32</sub> H <sub>38</sub> O <sub>14</sub>	Sagittatoside B
15	30.47	(M-H)-	529.17163	529.17043	0.287	C <sub>27</sub> H <sub>30</sub> O <sub>11</sub>	Baohuoside C
16	30.47	(M-H)-	721.23596	721.23382	3.895	C <sub>34</sub> H <sub>42</sub> O <sub>17</sub>	Icariin
17	32.88	(M-H)-	529.17194	529.17043	0.060	C <sub>27</sub> H <sub>30</sub> O <sub>11</sub>	Icariin I
18	34.36	(M-H)-	631.20447	631.20213	0.132	C <sub>31</sub> H <sub>36</sub> O <sub>14</sub>	Icariin F
19	34.71	(M-H)-	499.16156	499.15987	0.454	C <sub>26</sub> H <sub>28</sub> O <sub>10</sub>	Icariside
20	39.09	(M-H)-	513.18706	513.17552	-0.338	C <sub>27</sub> H <sub>30</sub> O <sub>10</sub>	Baohuoside I

RT, retention time; ppm, parts per million.

## Results

*Identification of active ingredients and potential targets of Epimedium.* Comparing the active ingredients in TGD that can enter the bloodstream, as identified by UHPLC-Q-Exactive Orbitrap HRMS in our previous study (11), a total of 20 active ingredients in *Epimedium* that could enter the rat bloodstream and exert their effects were identified, including Epimedin C, Epimedin B and others (Table I). The total ion chromatograms of active ingredients within *Epimedium* compound are displayed in Fig. 1.

To compensate for the lack of recent updates in drug databases, which may result in incomplete inclusion of components, network pharmacological analysis (using AD as an example) was conducted in conjunction with MS. Using 'Epimedium' as the key word, and oral bioavailability  $\geq 30\%$  and drug similarity  $\geq 0.18$  as the screening criteria in TCMSP, SwissTarget, PharmMapper and HERB databases, a total of 23 components of *Epimedium* were obtained, and 379 drug targets were retrieved. Using 'Alzheimer's disease' as the key word, a total of 1,165 drug targets were obtained from the GeneCards, DisGeNet and OMIM databases after deduplication. Based on the Venn diagram, 108 common targets of *Epimedium* and AD were identified (Fig. 2).

*Preventive effect of Epimedin C on H<sub>2</sub>O<sub>2</sub>-induced oxidative damage in PC12 cells.* H<sub>2</sub>O<sub>2</sub> stimulation can cause OS

damage, leading to apoptosis or necrosis in PC12 cells (35,36). Except for the control group, all the other groups of PC12 cells were exposed to 150  $\mu$ M H<sub>2</sub>O<sub>2</sub> treatment for 4 h for modeling OS (25). Before treatment with H<sub>2</sub>O<sub>2</sub>, these cells were pretreated with 0-160  $\mu$ M Epimedin C (Fig 3A) for 24 h to evaluate the protective effects of Epimedin C on PC12 cells and to identify its optimal concentration range for improving OS status (Fig. 3B). The results showed that 0-80  $\mu$ M Epimedin C pretreatment in PC12 cells did not have an effect on the viability of PC12 cells compared with the control. Among these concentrations, Epimedin C at concentrations of 1, 5 and 10  $\mu$ M had an improved cell survival rate than other concentrations; however, this was not statistically significant. Therefore, the concentrations of 1, 5 and 10  $\mu$ M were used for subsequent experiments. Relative to the OS model group, after 24 h of intervention with 17 $\beta$ -E2 and Epimedin C, the viability of PC12 cells was significantly improved (Fig. 3C). Among them, the cell survival rate significantly rose in a dose-dependent manner in response to pretreatment with 1, 5 and 10  $\mu$ M Epimedin C. LDH analysis was applied to detect the toxicity of different treatments on PC12 cells in each group; according to the results, relative to the control group, the H<sub>2</sub>O<sub>2</sub>-induced group showed a significant increase in LDH release (Fig. 3D). Alternatively, the cells pretreated with Epimedin C and 17 $\beta$ -E<sub>2</sub> displayed a significant decrease in LDH secretion and cytotoxicity compared with those in the H<sub>2</sub>O<sub>2</sub>-induced group. These comprehensive results indicated that intervention with 10  $\mu$ M

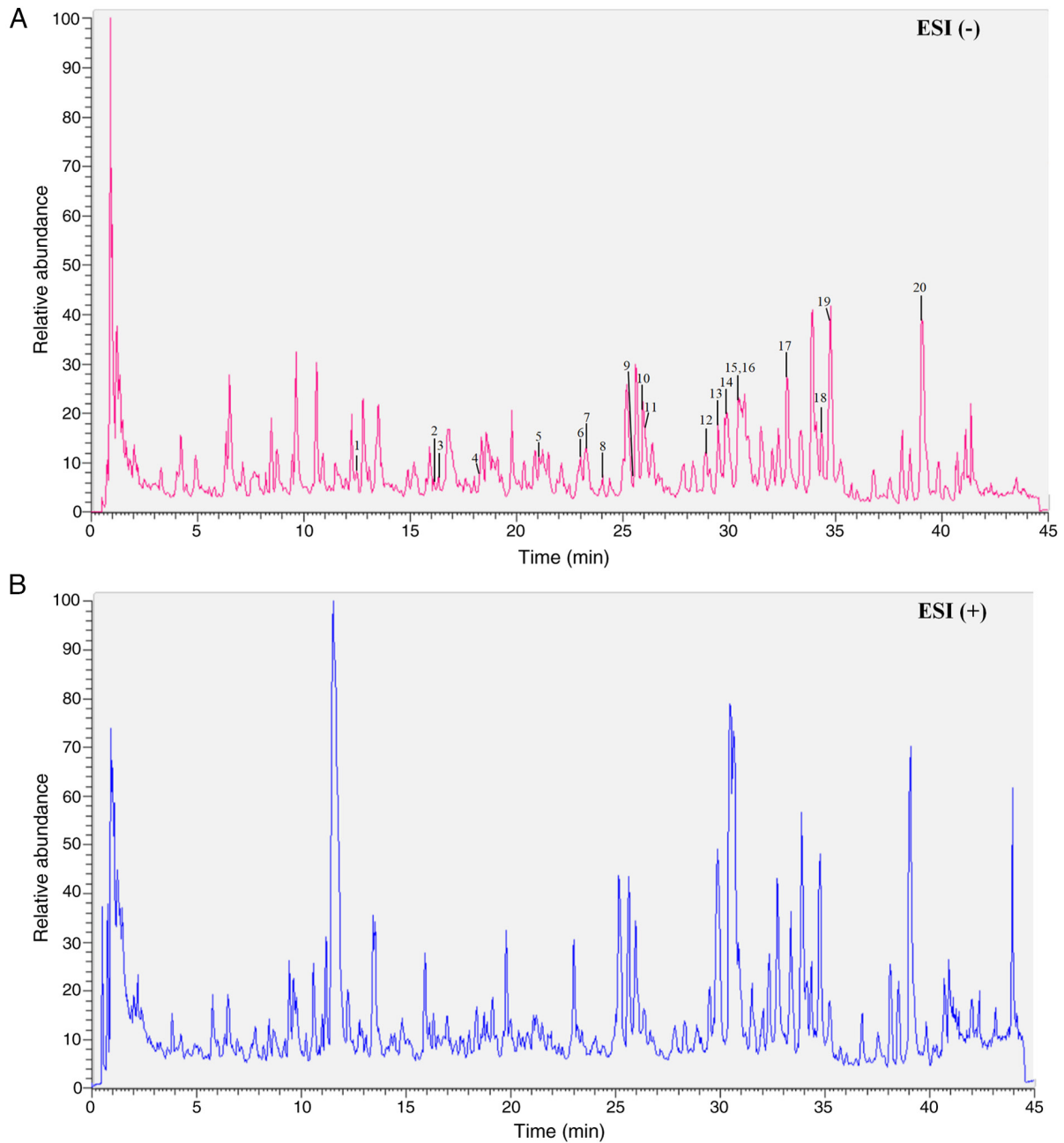


Figure 1. Total ion chromatograms in (A) negative and (B) positive ion modes of *Epimedium* identified by ultra-high performance liquid chromatography-quadrupole-Exact Orbitrap high resolution mass spectrometry.

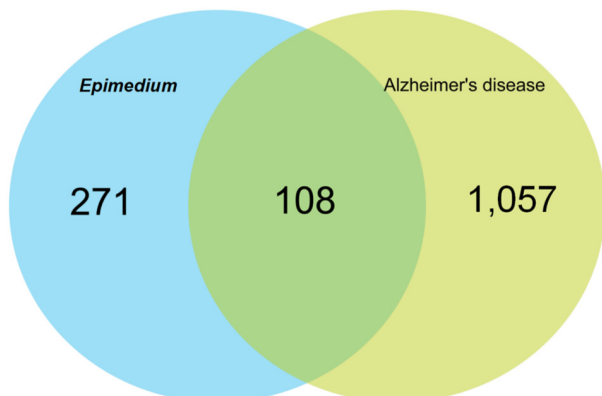


Figure 2. Venn diagram. Intersection targets of *Epimedium* and Alzheimer's disease.

*Epimedium* C had the best therapeutic efficacy in PC12 cell survival and the least toxic side effects.

**MDA and ROS levels.** MDA and ROS are involved in producing OS free radicals and are key indicators for measuring oxidative and antioxidant capacity (37,38). The results of the present study revealed that relative to the control group, MDA and ROS contents in PC12 cells induced by  $H_2O_2$  were significantly increased (Fig. 3E and F). In cells that had been pretreated with  $17\beta$ -E2 or 1, 5 and 10  $\mu$ M *Epimedium* C, the MDA and ROS contents were reduced to varying degrees compared with those in the  $H_2O_2$  group, indicating that *Epimedium* C is beneficial for alleviating the OS status of PC12 cells. Notably, 10  $\mu$ M *Epimedium* C was the most effective concentration.

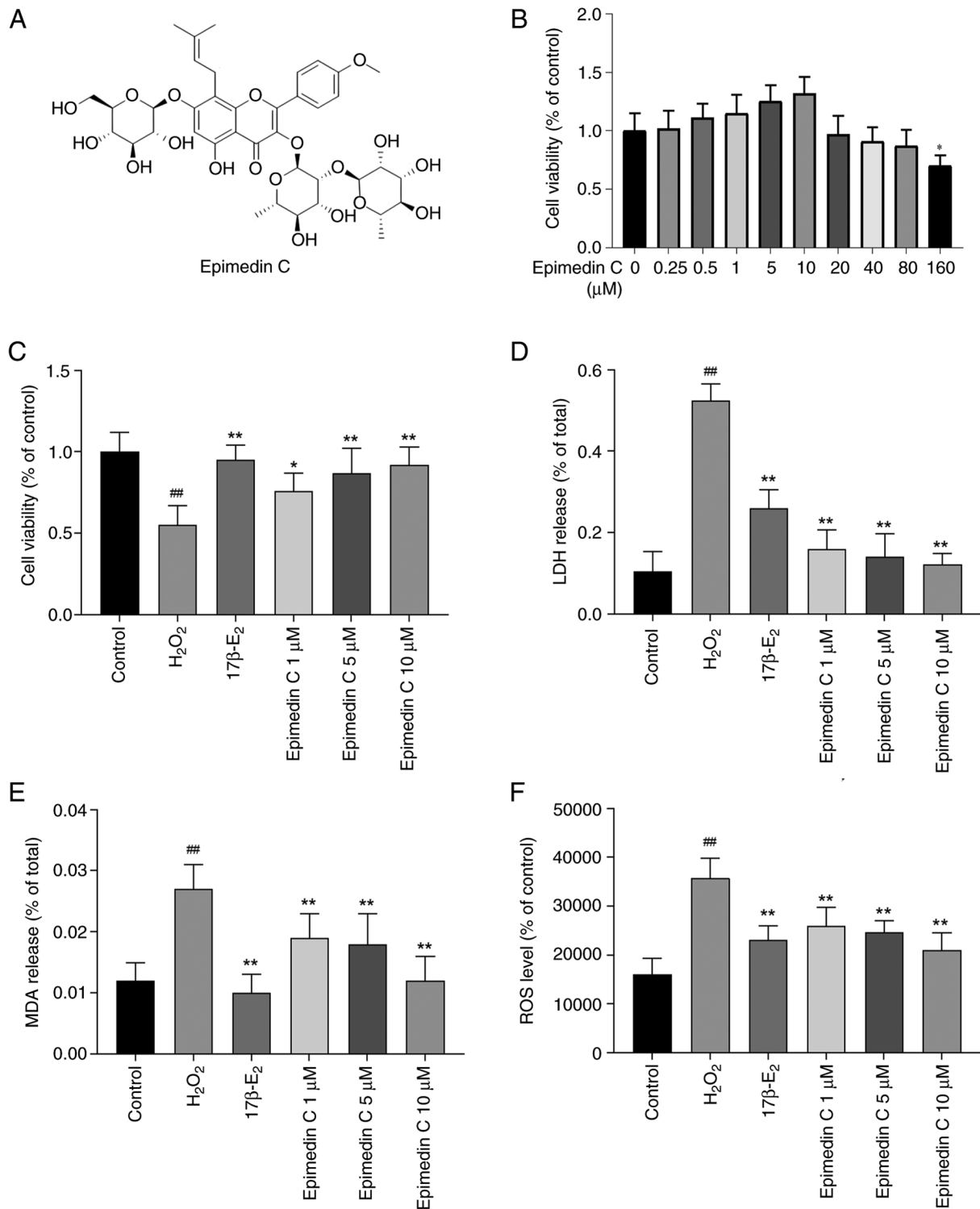


Figure 3. Epimedin C improves PC12 cell viability and protects against oxidative damage (A) Molecular structure of Epimedin C. (B) Comparison of cell viability of PC12 cells treated with different concentrations of Epimedin C. (C) Cell viability of PC12 cells in response to different intervention measures. Comparison of (D) LDH release, (E) MDA contents and (F) ROS levels in PC12 cells among the different treatment groups. Data are presented as the mean ± SD from six replicates. ##P<0.01 vs. control group; \*P<0.05, \*\*P<0.01 vs. H<sub>2</sub>O<sub>2</sub> group. 17β-E<sub>2</sub>, 17β-estradiol; LDH, lactate dehydrogenase; MDA, malondialdehyde.

Epimedin C can inhibit the H<sub>2</sub>O<sub>2</sub>-mediated apoptosis of PC12 cells. OS can induce cell apoptosis associated with increased ROS production and decreased MMP levels (39). Therefore, the cells were stained with Annexin V-FITC and PI, and the apoptosis rate was measured using flow cytometry (Fig. 4A and B). The present results showed that, after treatment with 150 μM

H<sub>2</sub>O<sub>2</sub> for 4 h, the PC12 cell apoptosis rate was significantly increased. By contrast, intervention with Epimedin C resulted in a decline in apoptosis rate compared with that in the H<sub>2</sub>O<sub>2</sub> group, suggesting that Epimedin C can inhibit cell apoptosis.

A reduction in MMP represents a hallmark event during early cell apoptosis, which is evident by the transition of

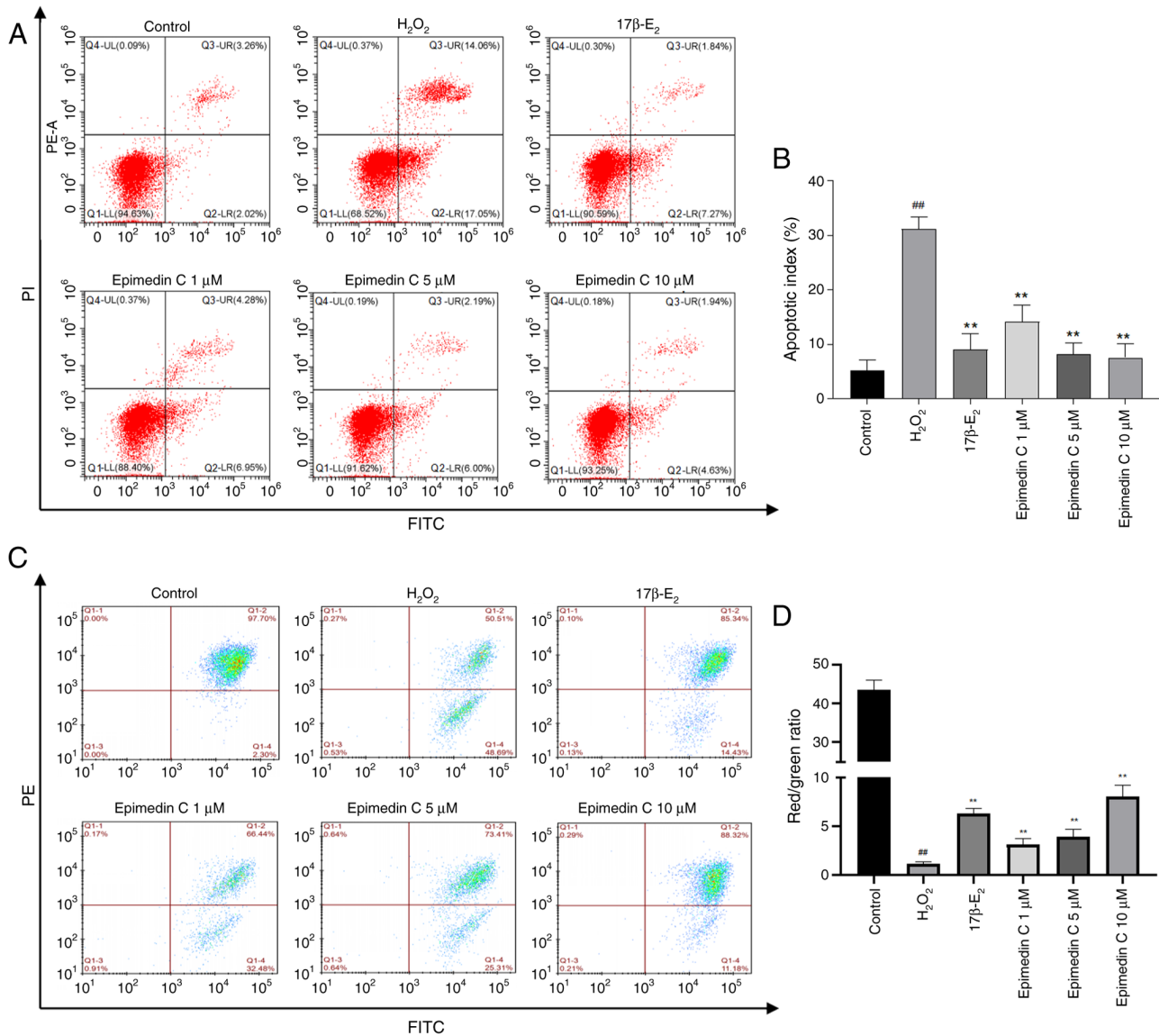


Figure 4. Flow cytometric analysis of apoptosis and MMP changes in PC12 cells (A) Apoptosis rate of each group of cells was detected by flow cytometry; cell populations stained with Annexin V-FITC and PI (quadrants 2 and 3) indicated apoptotic cells. (B) Summary of comparisons of apoptosis between groups. (C) JC-1 staining: Determination of MMP in each group of cells using flow cytometry. (D) MMP was determined by red/green fluorescence ratio. Data are presented as the mean  $\pm$  SD from three replicates. <sup>##</sup> $P < 0.01$  vs. control group; <sup>\*</sup> $P < 0.01$  vs. H<sub>2</sub>O<sub>2</sub> group. 17β-E<sub>2</sub>, 17β-estradiol; MMP, mitochondrial membrane potential.

JC-1 from red fluorescence to green fluorescence (40). To further evaluate the apoptosis status of each group of cells, the MMP loss within H<sub>2</sub>O<sub>2</sub>-treated PC12 cells was observed through JC-1 staining. As shown in Fig. 4C and D, the MMP of H<sub>2</sub>O<sub>2</sub>-treated PC12 cells was decreased, whereas pretreatment with Epimedine C (1, 5 and 10 μM) resulted in a dose-dependent improvement in MMP, with varying degrees of upregulation.

TUNEL staining can be conducted to detect apoptotic cells with large amounts of DNA degradation during the late stage of apoptosis (41). Therefore, TUNEL staining was performed on each group of cells in the current study (Fig. 5A). The results of the TUNEL assay revealed that relative to the control group, following H<sub>2</sub>O<sub>2</sub> induction modeling, the apoptosis of PC12 cells in the model group (level of red fluorescence) was significantly increased (Fig. 5B). Relative to the model group, after drug intervention, the apoptosis rates of PC12 cells in the 17β-E<sub>2</sub> and Epimedine C groups were significantly improved.

The degree of apoptosis was ameliorated to varying degrees in response to different concentrations of Epimedine C, with the largest improvement observed in the 10 μM Epimedine C group.

**Ultrastructural changes of PC12 cells.** Within the present study ultrastructural changes of PC12 cells in each group was observed using TEM (Fig. 6). Under physiological conditions, the mitochondria are present with prominent cristae and intact membranes (42). The control group cells had clear nuclear membranes and uniform chromatin. After H<sub>2</sub>O<sub>2</sub> induction, marked mitochondrial damage was observed in PC12 cells, evident as mitochondrial membrane rupture and chromatin condensation, accompanied by vacuolization. As aforementioned, 10 μM Epimedine C had the largest effect on improving H<sub>2</sub>O<sub>2</sub>-mediated OS damage to PC12 cells. Accordingly, TEM was performed on PC12 cells treated with 10 μM Epimedine

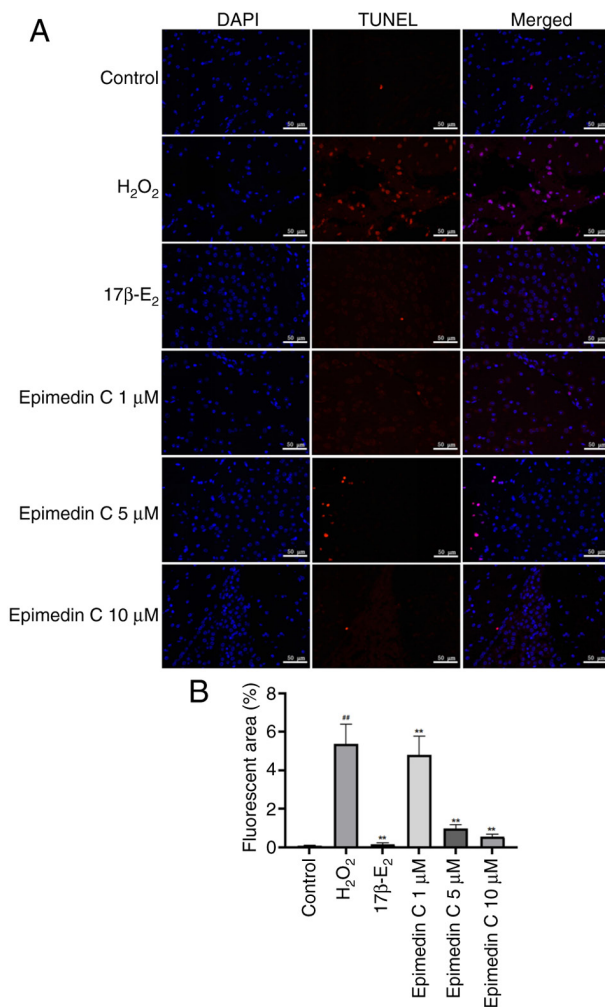


Figure 5. Comparison of cell apoptosis, detected by TUNEL staining, among the different groups. (A) Representative immunofluorescence images of TUNEL (red) and DAPI (blue) staining, and merged images. Scale bar, 50  $\mu\text{m}$  (n=5). (B) Summary of the fluorescent area for each treatment group. All results are presented as the mean  $\pm$  SD from five replicates. \*\*P<0.01 vs. control group; \*\*P<0.01 vs. H<sub>2</sub>O<sub>2</sub> group. 17 $\beta$ -E<sub>2</sub>, 17 $\beta$ -estradiol.

C to detect ultrastructural changes. The results indicated that treatment with 10  $\mu\text{M}$  Epimedin C could inhibit mitochondrial damage and alleviate mitochondrial swelling in PC12 cells, indicating that 10  $\mu\text{M}$  Epimedin C can improve oxidative damage and inhibit cell apoptosis.

*Roles of Epimedin C in activating the JNK/Nrf2/HO-1 pathway within H<sub>2</sub>O<sub>2</sub>-mediated PC12 cells.* The ‘drug-disease-target’ network was visualized with Cytoscape 3.8.2 software, and common targets between drugs (*Epimedium*) and diseases (AD) were imported in STRING database for PPI analysis. The PPI results included 110 nodes and 2,102 edges (Fig. 7A and B). Thereafter, the top 20 core genes of *Epimedium* for treating AD were screened using R language (R 4.1.2), including BCL2, APP, JUN, CASP3, ESR1, IL1B and TNF. The top 20 core targets underwent GO analysis in Metascape database. As a result, the shared targets were involved in various GO biological processes (Fig. 7D), including ‘positive regulation of apoptotic process’, ‘regulation of apoptotic signaling pathway’, ‘regulation of inflammatory

response’ and ‘cellular response to nitrogen compound’. Moreover, the GO molecular functional results (Fig. 7E) showed that the shared targets involved in ‘DNA-binding transcription factor binding’, ‘cytokine receptor binding’, ‘protease binding’ and ‘protein kinase binding’. While GO cellular component results (Fig. 7F) indicated that the shared targets were closely related to ‘platelet alpha granule lumen’, ‘neuronal cell body’, ‘transcription regulator complex’ and ‘receptor complex’. Additionally, as revealed by KEGG enrichment analysis, the shared targets were enriched in pathways such as ‘MAPK signaling pathway’, ‘endocrine resistance’, cell clearance and ‘apoptosis’ (Fig. 7C).

JNK belongs to the MAPK family and has a crucial effect on cell proliferation, differentiation, apoptosis, immune response and embryonic development (43). From the network pharmacological analysis, KEGG enrichment analysis showed that the pathway through which *Epimedium* improves AD was significantly enriched with the ‘MAPK signaling pathway’. In addition, the PPI network revealed that the top 20 core targets included APP, JUN and BCL2. Notably, JUN (also known as C-JUN) is involved in the JNK pathway (44), and activated JUN promotes the expression of various pro-apoptotic proteins (45). The Nrf2 pathway is an important regulatory factor for cellular antioxidant response (46), which is involved in triggering the expression of antioxidant and cell protective genes, and enhancing cellular antioxidant capacity (47); therefore, activation of Nrf2 can reduce neuronal damage caused by OS and inflammation (48). The free Nrf2 then transfers to the nucleus and binds to antioxidant-related elements, leading to the expression of various antioxidant and detoxifying genes, such as HO-1 (49). Research has shown that MAPKs are closely interrelated with Nrf2 nuclear translocation in eliminating OS (50).

Therefore, to study the neuroprotective role mediated by Epimedin C, WB was conducted for verifying p-JNK, Nrf2 and HO-1 protein levels. Relative to the control group, H<sub>2</sub>O<sub>2</sub> increased p-JNK levels but decreased Nrf2 levels, whereas Epimedin C downregulated p-JNK expression, and upregulated Nrf2 and HO-1 levels induced by H<sub>2</sub>O<sub>2</sub> (Fig. 8A-D). Furthermore, it was observed that compared with in the H<sub>2</sub>O<sub>2</sub> model group, Epimedin C decreased Bax expression while increasing Bcl-2 expression (Fig. 8A and E).

To confirm that Epimedin C mediated protection via the JNK pathway, the present study used a JNK agonist (anisomycin) for supplementary validation. The results revealed that p-JNK was activated and significantly upregulated in PC12 cells co-cultured with JNK agonist (Fig. 8F and H). By contrast, after treatment with Epimedin C and anisomycin, p-JNK expression decreased compared with following treatment with anisomycin alone, whereas Nrf2 and HO-1 levels were significantly increased (Fig. 8F-I).

## Discussion

With the aging population, neurodegenerative diseases are receiving increasing attention from the fields of science and medicine (51). According to statistics, in 2016, 5.4 million Americans suffered from AD (52), and based on further data published in 2021, it is estimated that >12 million Americans may develop neurodegenerative diseases over the

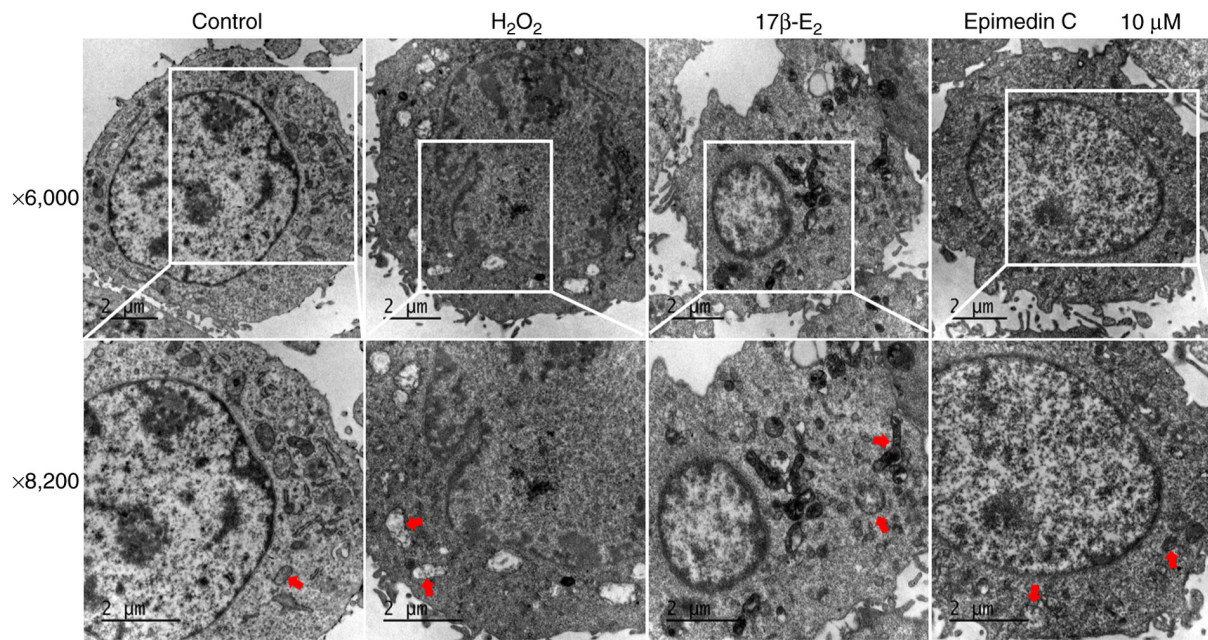


Figure 6. Transmission electron microscopy. Comparison of the ultrastructure of PC12 cells in different groups. Red arrows indicate mitochondria.  $17\beta\text{-E}_2$ ,  $17\beta$ -estradiol.

next 30 years (52). Neurodegenerative diseases are the main chronic progressive diseases that affect individual physical health (53), which exhibit the typical features of gradual selective neuronal system loss (54). OS can damage the blood-brain barrier (BBB), and as a result, neurotoxic substances can enter the brain and ultimately result in the accumulation of ROS (55). Upregulation of ROS levels has been confirmed to be a common major feature within the brains of patients with neurodegenerative disease (56), with excessive production of ROS causing ATP loss, decreased MMP and increased apoptosis (57). TCM has been used for treating neurodegenerative diseases for thousands of years (58), and according to a number of modern pharmacological studies, prescriptions, herbs, bioactive ingredients and monomeric compounds of TCM are effective at treating neurodegenerative diseases (59-61).

*Epimedium* is a TCM that is mainly applied in treating Parkinson's disease and AD (62). Research has confirmed that *Epimedium* has a protective effect on neurodegenerative diseases such as AD (19), and the active ingredients of *Epimedium* are flavonoids, which regulate various biological effects *in vitro* and *in vivo*, such as angiogenesis, antioxidant damage and inhibition of apoptosis (22,63). According to relevant research, icariin possesses antioxidant and immunomodulatory effects, and can regulate neuroendocrine function (64). It has been determined that 100 g/l *Epimedium* C is found to yield ~34.24 g/l icariin within 8 h (65). Compared with icariin, *Epimedium* C has a lower cost and comparable efficacy (21,65), and is an effective antioxidant. At present, to the best of our knowledge, no studies have yet been performed on *Epimedium* C and its specific mechanism in preventing and/or treating neurodegenerative diseases, including AD.

There is evidence to suggest that in AD, a vicious cycle revolves around the production of  $A\beta$ ,  $A\beta$  aggregation, plaque formation, microglia/immune response, inflammation and ROS production. In this cycle, ROS serves a central

role and  $\text{H}_2\text{O}_2$  is considered an important second messenger of ROS (66). The excessive production of  $\text{H}_2\text{O}_2$  can lead to OS and inflammation in the brain of patients with AD (67); therefore, it is considered that  $\text{H}_2\text{O}_2$  can simulate the disease manifestations of AD-related oxidative damage, and some studies have confirmed this (68,69). The present study confirmed that *Epimedium* C intervention enhanced cell viability and survival rate, improved OS damage caused by  $\text{H}_2\text{O}_2$  exposure and reduced the  $\text{H}_2\text{O}_2$ -mediated LDH leakage in PC12 cells. In the body, oxygen free radicals can be generated via both enzymatic and non-enzymatic systems, and the antioxidant defense system balances their levels; notably, if the biochemical balance between oxidants and antioxidants is disrupted, OS will occur (70). The increase in ROS content can disrupt the basic structures of proteins, nucleic acids and lipids, resulting in structural damage and functional changes, ultimately resulting in cell apoptosis (71). MDA is the final product of the oxidative decomposition of lipid peroxides, and its content can be measured to identify the degree of lipid peroxidation on the cell membrane (72). Therefore, the activities of superoxide dismutase and MDA are considered to be indicative of the degree of OS. The experimental results of the present study indicated that *Epimedium* C effectively reduced ROS accumulation mediated by  $\text{H}_2\text{O}_2$  within PC12 cells and lowered the levels of MDA after  $\text{H}_2\text{O}_2$  treatment, demonstrating its ability to resist OS. In addition, flow cytometry, TUNEL staining and MMP results all showed that PC12 cells underwent significant apoptosis after  $\text{H}_2\text{O}_2$  induction, and *Epimedium* C intervention had an inhibitory effect on cell apoptosis, with the best effect observed in responses to  $10\ \mu\text{M}$ . Under TEM, the PC12 cell ultrastructure also confirmed this: The mitochondrial membrane of PC12 cells was ruptured and chromatin was condensed, showing vacuolization and apoptosis after  $\text{H}_2\text{O}_2$  intervention. However, mitochondrial damage was notably reduced after intervention with  $10\ \mu\text{M}$

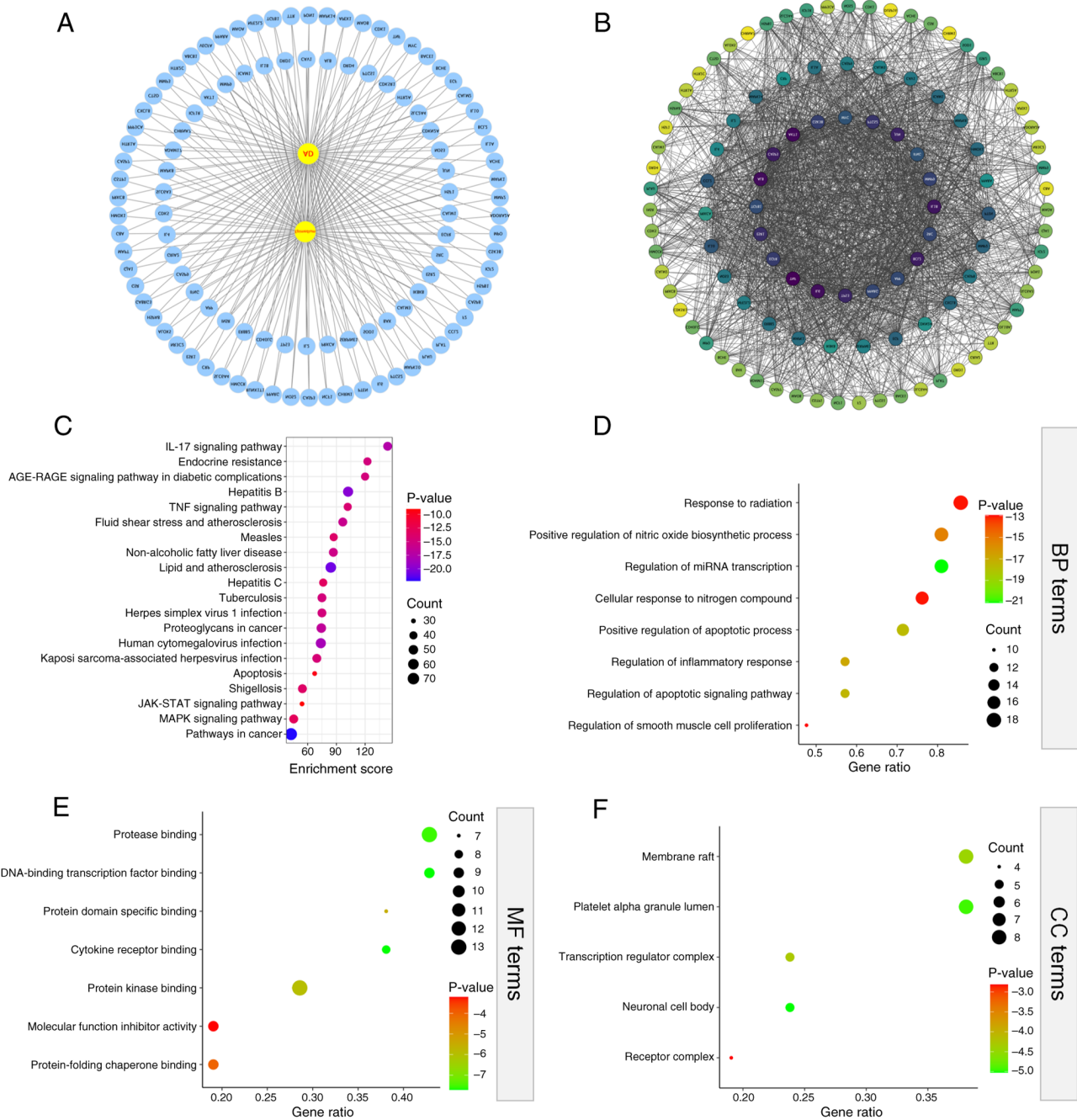


Figure 7. PPI network and functional enrichment analysis. (A) Network diagram of 'drug disease target'. (B) PPI common target gene network. (C) Kyoto Encyclopedia of Genes and Genomes analysis. Gene Ontology analysis: (D) BP terms, (E) MF terms and (F) CC terms. PPI, protein-protein interaction; BP, biological processes; MF, molecular functions; CC, cellular components.

Epimedin C. Therefore, it was hypothesized that Epimedin C has potential therapeutic effects on preventing and improving neurodegenerative diseases.

To seek the key targets and potential mechanisms of Epimedin C in improving neurodegenerative diseases, the present study first identified the active ingredients of *Epimedium* through UHPLC-Q-Exactive Orbitrap HRMS analysis and conducted network pharmacological analysis using AD as an example. A total of 108 shared targets were screened, and the top 20 core targets included APP, JUN and BCL2. From GO and KEGG analyses, the potential mechanism of *Epimedium* in improving AD was significantly

enriched in 'neuronal cell body', 'regulation of apoptotic signaling pathway' and 'MAPK signaling pathway'. MAPKs are conserved signaling proteins responsible for regulating numerous eukaryotic processes (73), and members of the MAPK family, including ERK1/2, JNK/SAPK, p38 and ERK5, are known to participate in neuron growth, differentiation and survival (74). JNK has an important effect on different diseases such as AD and Parkinson's disease caused by inflammation and OS (75), and research has confirmed that JNK pathway activation can exacerbate OS, leading to neurotoxic effects (76). Nrf2 is considered the main regulator of redox balance, which has a crucial role in cellular defense

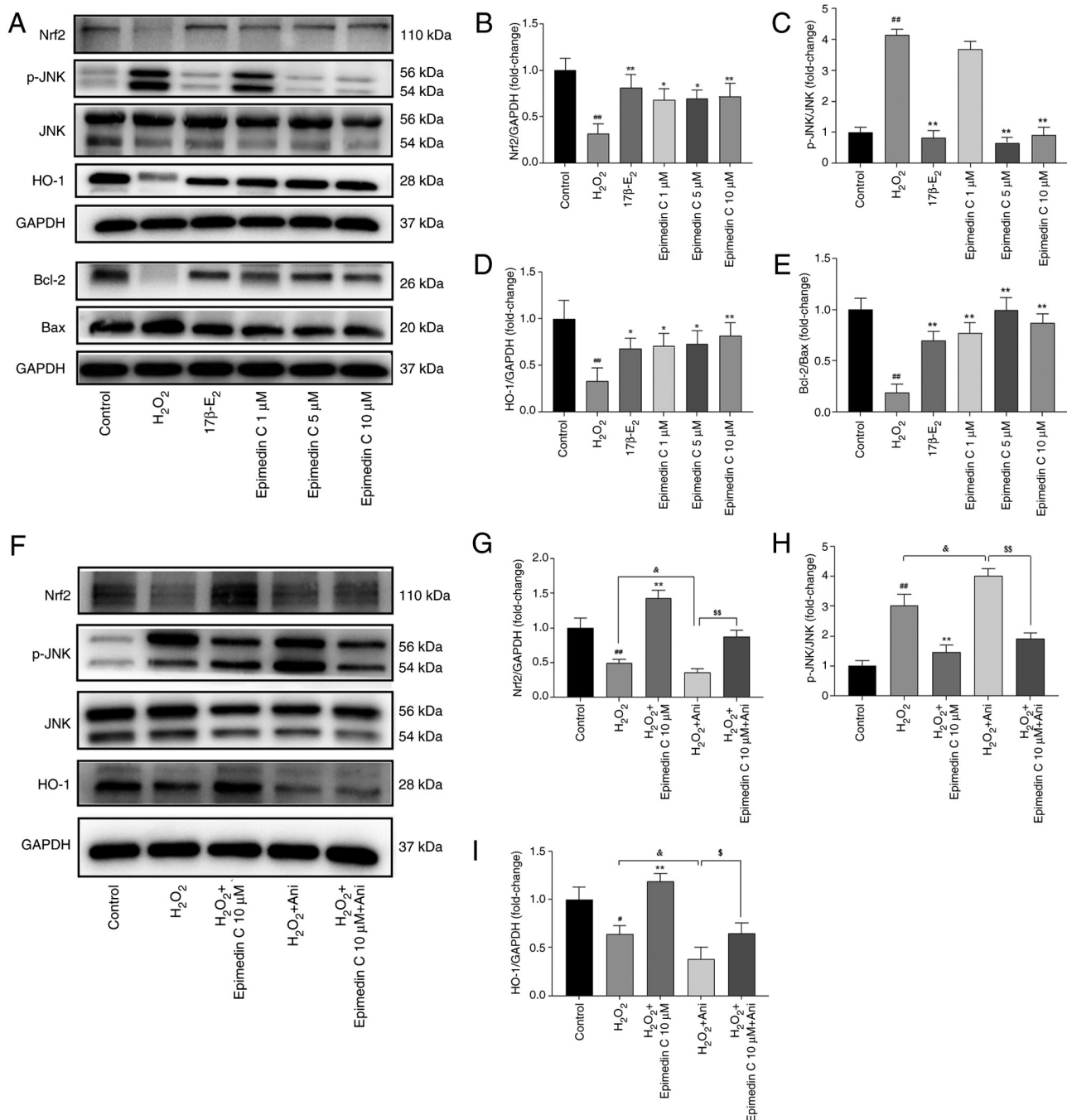


Figure 8. Effect of Epimedin C on the JNK/Nrf2/HO-1 signaling pathway and related protein levels detected by western blot analysis. (A) Western blot analysis of PC12 cells in each group (n=3). Semi-quantitative analysis of (B) Nrf2/GAPDH; (C) p-JNK/JNK; (D) HO-1/GAPDH; (E) Bcl-2/Bax. (F) Western blot analysis of PC12 cells in each group after JNK agonist (5 μM Ani) intervention (n=3). Semi-quantitative analysis of (G) Nrf2/GAPDH; (H) p-JNK/JNK; (I) HO-1/GAPDH. All results are presented as the mean ± SD from three replicates. \*P<0.05; #P<0.05, ##P<0.01 vs. control group; \*P<0.05, \*\*P<0.01 vs. H<sub>2</sub>O<sub>2</sub> group; †P<0.05, ††P<0.01 as indicated. 17β-E<sub>2</sub>, 17β-estradiol; Ani, anisomycin; HO-1, heme oxygenase-1; Nrf2, nuclear factor erythroid 2-related factor 2; p-, phosphorylated.

against OS (77,78). Research has shown that Nrf2/HO-1 expression is directly influenced by the JNK pathway, and activation of Nrf2/HO-1 signaling is crucial for reducing oxidative damage (79). Notably, our previous studies (80,81) have focused on validating the mechanism of action of the JNK pathway in response to TGD, particularly linking the JNK pathway to neuroprotection/neurodegeneration and OS response. One of these previous studies (25) confirmed that TGD can provide neuroprotective effects on H<sub>2</sub>O<sub>2</sub>-mediated

oxidative damage and apoptosis of PC12 cells through the Nrf2 and JNK pathways. *Epimedium* is the main drug component of TGD, and the aforementioned results offer a biological background and scientific foundation for the present study. Therefore, the present study focused on the JNK pathway to verify whether Epimedin C exerted neuroprotective effects through this pathway.

TGD has also been validated to improve premature menopause-associated cognitive dysfunction by increasing

estrogen levels (11). In addition, other *in vitro* and *in vivo* studies have supported the neuroprotective effects of estrogen and its effects on neurotransmitter systems related to cognition (25,80-82). When treating neurological diseases, the efficacy of oral TCM is determined by the ability of the components to reach target organs via the BBB (80). It is important to comprehensively understand serum pharmacokinetics of oral TCM to elucidate the absorption, distribution, metabolism and excretion of such active ingredients (83). According to research, active ingredients in TCM, such as *Epimedium*, can potentially improve BBB function, elevate cerebral blood flow and avoid cognitive impairment through suppressing the activation of astrocytes and microglia, protecting the myelin function of oligodendrocytes and reducing neuronal apoptosis (84). Furthermore, there is evidence suggesting that icariin exerts neuroprotection through crossing the BBB and regulating pathways (85). In our previous study, UHPLC-Q-Exactive Orbitrap HRMS was used to identify the components absorbed by mouse brain tissue after oral administration of TGD, in order to clarify the specific components that exert their effects on the brain. The results showed that icariin C could penetrate the BBB and exert therapeutic effects on the brain (11). A previous study reported that Epimedin C can be converted into icariin *in vivo* and gradually hydrolyzed into metabolic small molecules such as icariin C to exert its effects (86). Wong *et al* (87) explored the pharmacokinetics of isoprenoid flavonoids after ingestion of standardized *Epimedium* extract and assessed their relationship with serum estrogenic kinetics. The results of this previous study revealed the potential estrogenic effects of *Epimedium* extract and suggested that isoprenoid flavonoids might be used to treat menopause and other diseases requiring estrogenic effects. Epimedin C has been confirmed to be a mature plant extract with estrogen-like activity (88). Estradiol has been proven to have neuroprotective effects on excitatory neurotoxicity, OS and apoptosis (89-91). Therefore, similar to previous studies, the present study used  $17\beta$ -E<sub>2</sub> as a positive control drug and compared its efficacy with Epimedin C.

In the present study, WB results showed that relative to the control group, the JNK pathway was significantly activated following H<sub>2</sub>O<sub>2</sub> exposure, and Nrf2 and HO-1 levels were significantly reduced. However, after Epimedin C intervention, p-JNK expression evidently decreased, whereas Nrf2 and HO-1 levels increased. At the same time, Epimedin C decreased the levels of Bax and upregulated Bcl-2 levels, indicating that Epimedin C may alleviate OS damage and inhibit the apoptosis of PC12 cells through suppressing JNK pathway phosphorylation and activating Nrf2/HO-1. To further confirm this, the JNK agonist anisomycin was employed in the present study to further activate the JNK pathway and observe the improvement results after Epimedin C intervention. The results signified that compared with in the control and H<sub>2</sub>O<sub>2</sub> groups, JNK was activated and markedly upregulated in PC12 cells co-cultured with JNK agonist (H<sub>2</sub>O<sub>2</sub> + anisomycin group). After treatment with Epimedin C (H<sub>2</sub>O<sub>2</sub> + anisomycin + Epimedin C group), p-JNK expression was decreased, and Nrf2 and HO-1 levels were increased, which further confirmed the present hypothesis. Notably, according to the network pharmacological

analysis performed in the current study, Epimedin C has the characteristics of targeting multiple molecules and complex signal transduction. In this exploration, only the inhibitory effect of Epimedin C on JNK pathway phosphorylation was investigated, which may activate Nrf2/HO-1 and suppress the OS-induced apoptosis of PC12 cells. However, whether Epimedin C has other preventive mechanisms against neurodegenerative diseases still needs to be explored. According to a previous cell experiment, the medicinal components of Epimedin C can be effectively utilized and also converted into icariin (21). Notably, the difference in solubility between Epimedin C and icariin results in a higher Epimedin C initial concentration (9.72 mg/l) than icariin at the same dose (7.86 mg/l), and the residual concentration of Epimedin C in cells is also higher than that of icariin (21). At present, there is still a lack of research on the absorption of Epimedin C in the human body after ingestion of *Epimedium*. Therefore, it is crucial to optimize and explore the optimal drug concentration in cells, and drug absorption into target cells is a prerequisite for the subsequent therapeutic effects (92). According to the results of the present study, Epimedin C at 160  $\mu$ M exerted neurotoxicity: Considering that *Epimedium* contains  $\sim 5 \mu$ M/g Epimedin C (93), it is speculated the human dosage of *Epimedium* should not exceed 32 g. A limitation of the present study is that only *in vitro* PC12 cell experiments were conducted. Due to the complexity and heterogeneity of human pathology, translating these findings into human therapies requires careful and robust validation through in-depth molecular research and comprehensive clinical trials (91). Future research will further conduct relevant clinical trials, focusing on the pharmacological mechanisms of Epimedin C in preventing neurodegenerative diseases *in vivo* and *in vitro*, aiming to offer a reliable scientific foundation for applying Epimedin C to exert neuroprotective effects and prevent neurodegenerative diseases.

In conclusion the present study revealed the neuroprotective mechanism of Epimedin C. To the best of our knowledge, the current findings are the first to indicate that Epimedin C can mediate the JNK/Nrf2/HO-1 pathway, providing protection from H<sub>2</sub>O<sub>2</sub>-mediated OS and apoptosis in PC12 cells. These findings suggest that Epimedin C may become a candidate drug for preventing neurodegenerative diseases. In the future, further exploration of the potential preventive mechanisms of Epimedin C in neurodegenerative diseases is needed to provide more reliable and direct scientific evidence.

#### Acknowledgements

Not applicable.

#### Funding

This work was supported by the National Natural Science Foundation of China (grant nos. 82174427 and 82305290).

#### Availability of data and materials

The data generated in the present study may be requested from the corresponding author.

## Authors' contributions

CC and XLL were involved in writing the original draft, and reviewing and editing the manuscript. CC was also responsible for data curation, software application and data analysis. XLL conceptualized and supervised the project. CC, XLL, and GYL performed the experiments. GYL was responsible for data analysis and software application. LWX was responsible for conceptualization, project administration and funding acquisition. GYL and LWX ultimately reviewed and edited the manuscript. CC, XLL, GYL and LWX confirm the authenticity of all the raw data, and read and approved the final manuscript. All authors agree to be accountable for all aspects of work ensuring integrity and accuracy.

## Ethics approval and consent to participate

Not applicable.

## Patient consent for publication

Not applicable.

## Competing interests

The authors declare that they have no competing interests.

## References

- Li R, Robinson M, Ding X, Geetha T, Al-Nakkash L, Broderick TL and Babu JR: Genistein: A focus on several neurodegenerative diseases. *J Food Biochem* 46: e14155, 2022.
- Bell SM, Burgess T, Lee J, Blackburn DJ, Allen SP and Mortiboys H: Peripherally glycolysis in neurodegenerative diseases. *Int J Mol Sci* 21: 8924, 2020.
- Kovacs GG: Molecular pathology of neurodegenerative diseases: Principles and practice. *J Clin Pathol* 72: 725-735, 2019.
- Varela L and Garcia-Rendueles MER: Oncogenic pathways in neurodegenerative diseases. *Int J Mol Sci* 23: 3223, 2022.
- Orfali R, Alwatban AZ, Orfali RS, Lau L, Chea N, Alotaibi AM, Nam YW and Zhang M: Oxidative stress and ion channels in neurodegenerative diseases. *Front Physiol* 15: 1320086, 2024.
- Chang KH, Cheng ML, Chiang MC and Chen CM: Lipophilic antioxidants in neurodegenerative diseases. *Clin Chim Acta* 485: 79-87, 2018.
- Finkel T and Holbrook NJ: Oxidants, oxidative stress and the biology of ageing. *Nature* 408: 239-247, 2000.
- Li Y, Li L and Hölscher C: Therapeutic potential of genipin in central neurodegenerative diseases. *CNS Drugs* 30: 889-897, 2016.
- Chen Q, Chen G and Wang Q: Application of network pharmacology in the treatment of neurodegenerative diseases with traditional Chinese medicine. *Planta Med* 91: 226-237, 2025.
- Wang SF, Wu MY, Cai CZ, Li M and Lu JH: Autophagy modulators from traditional Chinese medicine: Mechanisms and therapeutic potentials for cancer and neurodegenerative diseases. *J Ethnopharmacol* 194: 861-876, 2016.
- Li XL, Lin ZH, Chen SR, Ni S, Lin GY, Wang W, Lin JY, Zhao Q, Cong C and Xu LW: Tiaogeng decoction improves mild cognitive impairment in menopausal APP/PS1 mice through the ERs/NF- $\kappa$ b/AQP1 signaling pathway. *Phytomedicine* 138: 156391, 2025.
- Yang X, Chen J, Huang W, Zhang Y, Yan X, Zhou Z and Wang Y: Synthesis of icariin in tobacco leaf by overexpression of a glucosyltransferase gene from *Epimedium sagittatum*. *Ind Crop Prod* 156: 112841, 2020.
- Li J, Yu Y, Zhang Y, Zhou Y, Ding S, Dong S, Jin S and Li Q: Flavonoids derived from Chinese Medicine: Potential neuroprotective agents. *Am J Chin Med* 52: 1613-1640, 2024.
- Zhou M, Zheng W, Sun X, Yuan M, Zhang J, Chen X, Yu K, Guo B and Ma B: Comparative analysis of chemical components in different parts of *Epimedium* Herb. *J Pharm Biomed Anal* 198: 113984, 2021.
- Zhang HF, Yang XH, Zhao LD and Wang Y: Ultrasonic-assisted extraction of epimedin C from fresh leaves of *Epimedium* and extraction mechanism. *Innovative Food Science & Emerging Technologies* 54-60: 1466-8564, 2009.
- Luo D, Shi D and Wen L: From epimedium to neuroprotection: Exploring the potential of wushanicaritin. *Foods* 13: 1493, 2024.
- Li XA, Ho YS, Chen L and Hsiao WL: The protective effects of icariin against the homocysteine-induced neurotoxicity in the primary embryonic cultures of rat cortical neurons. *Molecules* 21: 1557, 2016.
- Chinese Pharmacopoeia Commission: Pharmacopoeia of the People's Republic of China. Vol 1. China Medical Science Press, Beijing, 2020.
- Wu L, Du ZR, Xu AL, Yan Z, Xiao HH, Wong MS, Yao XS and Chen WF: Neuroprotective effects of total flavonoid fraction of the *Epimedium koreanum* Nakai extract on dopaminergic neurons: In vivo and in vitro. *Biomed Pharmacother* 91: 656-663, 2017.
- Zhang HF, Yang TS, Li ZZ and Wang Y: Simultaneous extraction of epimedin A, B, C and icariin from *Herba Epimedii* by ultrasonic technique. *Ultrason Sonochem* 15: 376-385, 2008.
- Huang X, Wang X, Zhang Y, Shen L, Wang N, Xiong X, Zhang L, Cai X and Shou D: Absorption and utilisation of epimedin C and icariin from *Epimedium* herba, and the regulatory mechanism via the BMP2/Runx2 signalling pathway. *Biomed Pharmacother* 118: 109345, 2019.
- Wei DH, Deng JL, Shi RZ, Ma L, Shen JM, Hoffman R, Hu YH, Wang H and Gao JL: Epimedin C protects H<sub>2</sub>O<sub>2</sub>-induced peroxidation injury by enhancing the function of endothelial progenitor HUVEC populations. *Biol Pharm Bull* 42: 1491-1499, 2019.
- Ohnuma K, Hayashi Y, Furue M, Kaneko K and Asashima M: Serum-free culture conditions for serial subculture of undifferentiated PC12 cells. *J Neurosci Methods* 151: 250-261, 2006.
- Cheng B, Lu H, Bai B and Chen J:  $\beta$ -D-Hydroxybutyrate inhibited the apoptosis of PC12 cells induced by H<sub>2</sub>O<sub>2</sub> via inhibiting oxidative stress. *Neurochem Int* 62: 620-625, 2013.
- Gao X, Li S, Liu X, Cong C, Zhao L, Liu H and Xu L: Neuroprotective effects of Tiaogeng decoction against H<sub>2</sub>O<sub>2</sub>-induced oxidative injury and apoptosis in PC12 cells via Nrf2 and JNK signaling pathways. *J Ethnopharmacol* 279: 114379, 2021.
- Zhao Y, Kuca K, Wu W, Wang X, Nepovimova E, Musilek K and Wu Q: Hypothesis: JNK signaling is a therapeutic target of neurodegenerative diseases. *Alzheimers Dement* 18: 152-158, 2022.
- Cho H and Hah JM: A perspective on the development of c-Jun N-terminal Kinase inhibitors as therapeutics for Alzheimer's disease: Investigating structure through docking studies. *Biomedicines* 9: 1431, 2021.
- Osama A, Zhang J, Yao J, Yao X and Fang J: Nrf2: A dark horse in Alzheimer's disease treatment. *Ageing Res Rev* 64: 101206, 2020.
- Wang M, Tong K, Chen Z and Wen Z: Mechanisms of 15-Epi-LXA4-Mediated HO-1 in cytoprotection following inflammatory injury. *J Surg Res* 281: 245-255, 2023.
- Atabaki MM, Ghotbeddin Z, Rahimi K and Tabandeh MR: The potential of alphapinene as a therapeutic agent for maternal hypoxia-induced cognitive impairments: A study on HO-1 and Nrf2 gene expression in rats. *Metab Brain Dis* 40: 112, 2025.
- Li J, Kuang G, Chen X and Zeng R: Identification of chemical composition of leaves and flowers from *paeonia rockii* by UHPLC-Q-exactive orbitrap HRMS. *Molecules* 21: 947, 2016.
- Lozan E, Shinkaruk S, Al Abed SA, Lamothe V, Potier M, Marigetto A, Schmitter JM, Bennetau-Pelissero C and Buré C: Derivatization-free LC-MS/MS method for estrogen quantification in mouse brain highlights a local metabolic regulation after oral versus subcutaneous administration. *Anal Bioanal Chem* 409: 5279-5289, 2017.
- Guglielmotto M, Reineri S, Iannello A, Ferrero G, Vanzan L, Miano V, Ricci L, Tamagno E, De Bortoli M and Cutrupi S: E2 regulates epigenetic signature on neuroglobin enhancer-promoter in neuronal cells. *Front Cell Neurosci* 10: 147, 2016.
- Singh P and Paramanik V: Neuromodulating roles of estrogen and phytoestrogens in cognitive therapeutics through epigenetic modifications during aging. *Front Aging Neurosci* 14: 945076, 2022.

35. Lin J, Wu J, Xu Y, Zhao Y and Ye S: RhFGF21 protected PC12 cells against mitochondrial apoptosis triggered by H<sub>2</sub>O<sub>2</sub> via the AKT-mediated ROS signaling pathway. *Exp Cell Res* 445: 114417, 2025.
36. Li Y, Long J, Li L, Yu Z, Liang Y, Hou B, Xiang L and Niu X: Pioglitazone protects PC12 cells against oxidative stress injury: An in vitro study of its antiapoptotic effects via the PPAR $\gamma$  pathway. *Exp Ther Med* 26: 522, 2023.
37. Cheng Y, Huang X, Tang Y, Li J, Tan Y and Yuan Q: Effects of evodiamine on ROS/TXNIP/NLRP3 pathway against gouty arthritis. *Naunyn Schmiedebergs Arch Pharmacol* 397: 1015-1023, 2024.
38. Abedi A, Ghobadi H, Sharghi A, Iranpour S, Fazlzadeh M and Aslani MR: Effect of saffron supplementation on oxidative stress markers (MDA, TAC, TOS, GPx, SOD, and pro-oxidant/antioxidant balance): An updated systematic review and meta-analysis of randomized placebo-controlled trials. *Front Med (Lausanne)* 10: 1071514, 2023.
39. Satoh T, Enokido Y, Aoshima H, Uchiyama Y and Hatanaka H: Changes in mitochondrial membrane potential during oxidative stress-induced apoptosis in PC12 cells. *J Neurosci Res* 50: 413-420, 1997.
40. Perelman A, Wachtel C, Cohen M, Haupt S, Shapiro H and Tzur A: JC-1: Alternative excitation wavelengths facilitate mitochondrial membrane potential cytometry. *Cell Death Dis* 3: e430, 2012.
41. Kyrylkova K, Kyryachenko S, Leid M and Kioussi C: Detection of apoptosis by TUNEL assay. *Methods Mol Biol* 887: 41-47, 2012.
42. Protasoni M and Zeviani M: mitochondrial structure and bioenergetics in normal and disease conditions. *Int J Mol Sci* 22: 586, 2021.
43. Wang G, Zhao Z, Ren B, Yu W, Zhang X, Liu J, Wang L, Si D and Yang M: Exenatide exerts a neuroprotective effect against diabetic cognitive impairment in rats by inhibiting apoptosis: Role of the JNK/c-JUN signaling pathway. *Mol Med Rep* 25: 111, 2022.
44. Kong R, Shi J, Xie K, Wu H, Wang X, Zhang Y and Wang Y: A study of JUN's promoter region and its regulators in chickens. *Genes (Basel)* 15: 1351, 2024.
45. Huang HM and Liu JC: c-Jun blocks cell differentiation but not growth inhibition or apoptosis of chronic myelogenous leukemia cells induced by ST1571 and by histone deacetylase inhibitors. *J Cell Physiol* 218: 568-574, 2009.
46. Chen F, Xiao M, Hu S and Wang M: Keap1-Nrf2 pathway: A key mechanism in the occurrence and development of cancer. *Front Oncol* 14: 1381467, 2024.
47. Galan-Cobo A, Sitthideatphaiboon P, Qu X, Poteete A, Pisegna MA, Tong P, Chen PH, Boroughs LK, Rodriguez MLM, Zhang W, *et al*: LKB1 and KEAP1/NRF2 pathways cooperatively promote metabolic reprogramming with enhanced glutamine dependence in KRAS-mutant lung adenocarcinoma. *Cancer Res* 79: 3251-3267, 2019.
48. Buendía I, Michalska P, Navarro E, Gameiro I, Egea J and León R: Nrf2-ARE pathway: An emerging target against oxidative stress and neuroinflammation in neurodegenerative diseases. *Pharmacol Ther* 157: 84-104, 2016.
49. Xiao Q, Piao R, Wang H, Li C and Song L: Orientin-mediated Nrf2/HO-1 signal alleviates H<sub>2</sub>O<sub>2</sub>-induced oxidative damage via induction of JNK and PI3K/AKT activation. *Int J Biol Macromol* 118 (Pt A): 747-755, 2018.
50. Feng L, Wu Y, Wang J, Han Y, Huang J and Xu H: Neuroprotective effects of a novel tetrapeptide SGGY from Walnut against H<sub>2</sub>O<sub>2</sub>-stimulated oxidative stress in SH-SY5Y cells: Possible involved JNK, p38 and Nrf2 signaling pathways. *Foods* 12: 1490, 2023.
51. Kuntiç M, Hahad O, Münzel T and Daiber A: Crosstalk between oxidative stress and inflammation caused by noise and air pollution-implications for neurodegenerative diseases. *Antioxidants (Basel)* 13: 266, 2024.
52. Downs BW, Kushner S, Bagchi M, Blum K, Badgaiyan RD, Chakraborty S and Bagchi D: Etiology of neuroinflammatory pathologies in neurodegenerative diseases: A treatise. *Curr Psychopharmacol* 10: 123-137, 2021.
53. Li Y, Zhang W, Zhang Q, Li Y, Xin C, Tu R and Yan H: Oxidative stress of mitophagy in neurodegenerative diseases: Mechanism and potential therapeutic targets. *Arch Biochem Biophys* 764: 110283, 2025.
54. Pardo-Díaz R, Pérez-García P, Castro C, Nunez-Abades P and Carrascal L: Oxidative stress as a potential mechanism underlying membrane hyperexcitability in neurodegenerative diseases. *Antioxidants (Basel)* 11: 1511, 2022.
55. Kim S, Jung UJ and Kim SR: Role of oxidative stress in blood-brain barrier disruption and neurodegenerative diseases. *Antioxidants (Basel)* 13: 1462, 2024.
56. Tarozzi A: Oxidative stress in neurodegenerative diseases: From preclinical studies to clinical applications. *J Clin Med* 9: 1223, 2020.
57. Shams Ul Hassan S, Ishaq M, Zhang WD and Jin HZ: An overview of the mechanisms of marine Fungi-derived anti-inflammatory and anti-tumor agents and their novel role in drug targeting. *Curr Pharm Des* 27: 2605-2614, 2021.
58. Cai Z, Liu M, Zeng L, Zhao K, Wang C, Sun T, Li Z and Liu R: Role of traditional Chinese medicine in ameliorating mitochondrial dysfunction via non-coding RNA signaling: Implication in the treatment of neurodegenerative diseases. *Front Pharmacol* 14: 1123188, 2023.
59. Mohd Sairazi NS and Sirajudeen KNS: Natural products and their bioactive compounds: Neuroprotective potentials against neurodegenerative diseases. *Evid Based Complement Alternat Med* 2020: 6565396, 2020.
60. Chen L, Liu Y and Xie J: The beneficial pharmacological effects of *Uncaria rhyncophylla* in neurodegenerative diseases: Focus on alkaloids. *Front Pharmacol* 15: 1436481, 2024.
61. Wang ZY, Liu J, Zhu Z, Su CF, Sreenivasmurthy SG, Iyaswamy A, Lu JH, Chen G, Song JX and Li M: Traditional Chinese medicine compounds regulate autophagy for treating neurodegenerative disease: A mechanism review. *Biomed Pharmacother* 133: 110968, 2021.
62. Chen XL, Li SX, Ge T, Zhang DD, Wang HF, Wang W, Li YZ and Song XM: *Epimedium* Linn: A comprehensive review of phytochemistry, pharmacology, clinical applications and quality control. *Chem Biodivers* 21: e202400846, 2024.
63. Li C, Li Q, Mei Q and Lu T: Pharmacological effects and pharmacokinetic properties of icariin, the major bioactive component in *Herba Epimedii*. *Life Sci* 126: 57-68, 2015.
64. Zong N, Li F, Deng Y, Shi J, Jin F and Gong Q: Icariin, a major constituent from *Epimedium brevicornum*, attenuates ibotenic acid-induced excitotoxicity in rat hippocampus. *Behav Brain Res* 313: 111-119, 2016.
65. Liu F, Wei B, Cheng L, Zhao Y, Liu X, Yuan Q and Liang H: Co-Immobilizing two glycosidases based on cross-linked enzyme aggregates to enhance enzymatic properties for achieving high titer Icaritin biosynthesis. *J Agric Food Chem* 70: 11631-11642, 2022.
66. Yang J, Yang J, Liang SH, Xu Y, Moore A and Ran C: Imaging hydrogen peroxide in Alzheimer's disease via cascade signal amplification. *Sci Rep* 6: 35613, 2016.
67. Gharai PK, Khan J, Mallesh R, Garg S, Saha A, Ghosh S and Ghosh S: Vanillin benzothiazole derivative reduces cellular reactive oxygen species and detects amyloid fibrillar aggregates in Alzheimer's disease brain. *ACS Chem Neurosci* 14: 773-786, 2023.
68. Sajjad N, Wani A, Sharma A, Ali R, Hassan S, Hamid R, Habib H and Ganai BA: *Artemisia amygdalina* Upregulates Nrf2 and protects neurons against oxidative stress in Alzheimer disease. *Cell Mol Neurobiol* 39: 387-399, 2019.
69. Zakharova IO, Sokolova TV, Furaev VV, Rychkova MP and Avrova NF: (Effects of oxidative stress inducers, neurotoxins, and ganglioside GM1 on Na<sup>+</sup>, K<sup>+</sup>-ATPase in PC12 and brain synaptosomes). *Zh Evol Biokhim Fiziol* 43: 148-154, 2007 (In Russian).
70. Demirci-Çekiç S, Özkan G, Avan AN, Uzunboy S, Çapanoğlu E and Apak R: Biomarkers of oxidative stress and antioxidant defense. *J Pharm Biomed Anal* 209: 114477, 2022.
71. Pisoschi AM and Pop A: The role of antioxidants in the chemistry of oxidative stress: A review. *Eur J Med Chem* 97: 55-74, 2015.
72. Zhang R, Guo X, Zhang Y and Tian C: Influence of modified atmosphere treatment on post-harvest reactive oxygen metabolism of pomegranate peels. *Nat Prod Res* 34: 740-744, 2020.
73. González-Rubio G, Sellers-Moya Á, Martín H and Molina M: A walk-through MAPK structure and functionality with the 30-year-old yeast MAPK Slt2. *Int Microbiol* 24: 531-543, 2021.
74. Miloso M, Scuteri A, Foudah D and Tredici G: MAPKs as mediators of cell fate determination: An approach to neurodegenerative diseases. *Curr Med Chem* 15: 538-548, 2008.
75. Du J, Wang G, Luo H, Liu N and Xie J: JNK-IN-8 treatment alleviates lipopolysaccharide-induced acute lung injury via suppression of inflammation and oxidative stress regulated by JNK/NF- $\kappa$ B signaling. *Mol Med Rep* 23: 150, 2021.

76. Li R, Yang W, Yan X, Zhou X, Song X, Liu C, Zhang Y and Li J: Folic acid mitigates the developmental and neurotoxic effects of bisphenol A in zebrafish by inhibiting the oxidative stress/JNK signaling pathway. *Ecotoxicol Environ Saf* 288: 117363, 2024.
77. Shakya A, McKee NW, Dodson M, Chapman E and Zhang DD: Anti-ferroptotic effects of Nrf2: Beyond the antioxidant response. *Mol Cells* 46: 165-175, 2023.
78. Hallis SP, Kim JM and Kwak MK: Emerging role of NRF2 signaling in cancer stem cell phenotype. *Mol Cells* 46: 153-164, 2023.
79. Huang SY, Chang SF, Chau SF and Chiu SC: The protective effect of hispidin against hydrogen peroxide-induced oxidative stress in ARPE-19 cells via Nrf2 signaling pathway. *Biomolecules* 9: 380, 2019.
80. Li S, Cong C, Liu Y, Liu X, Liu H, Zhao L, Gao X, Gui W and Xu L: Tiao Geng decoction inhibits tributyltin chloride-induced GT1-7 neuronal apoptosis through ASK1/MKK7/JNK signaling pathway. *J Ethnopharmacol* 269: 113669, 2021.
81. Li S, Cong C, Liu Y, Liu X, Kluwe L, Shan X, Liu H, Gao M, Zhao L, Gao X and Xu L: Tiao Geng decoction for treating menopausal syndrome exhibits anti-aging effects likely via suppressing ASK1/MKK7/JNK mediated apoptosis in ovariectomized rats. *J Ethnopharmacol* 261: 113061, 2020.
82. Ryan J, Scali J, Carriere I, Ritchie K and Ancelin ML: Hormonal treatment, mild cognitive impairment and Alzheimer's disease. *Int Psychogeriatr* 20: 47-56, 2008.
83. Li C, Jia WW, Yang JL, Cheng C and Olaleye OE: Multi-compound and drug-combination pharmacokinetic research on Chinese herbal medicines. *Acta Pharmacol Sin* 43: 3080-3095, 2022.
84. Chen L, Zhen Y, Wang X, Wang J and Zhu G: Neurovascular glial unit: A target of phytotherapy for cognitive impairments. *Phytomedicine* 119: 155009, 2023.
85. Sharma S, Mehan S, Khan Z, Tiwari A, Kumar A, Gupta GD, Narula AS and Kalfin R: Exploring the neuroprotective potential of icariin through modulation of neural pathways in the treatment of neurological diseases. *Curr Mol Med*: Sep 26, 2024 (Epub ahead of print).
86. Zhang Y, Wang Y, Zhang X, Liu Y, Li J and Wang J: Metabolic profiling of epimedidin C in Rats: In vivo and in vitro studies. *Front. Pharmacol* 9: 456, 2018.
87. Wong SP, Shen P, Lee L, Li J and Yong EL: Pharmacokinetics of prenylflavonoids and correlations with the dynamics of estrogen action in sera following ingestion of a standardized Epimedium extract. *J Pharm Biomed Anal* 50: 216-223, 2009.
88. Xie L, Zhao S, Zhang X, Huang W, Qiao L, Zhan D, Ma C, Gong W, Dang H and Lu H: Wenshenyang recipe treats infertility through hormonal regulation and inflammatory responses revealed by transcriptome analysis and network pharmacology. *Front Pharmacol* 13: 917544, 2022.
89. Hara Y, Waters EM, McEwen BS and Morrison JH: estrogen effects on cognitive and synaptic health over the lifecourse. *Physiol Rev* 95: 785-807, 2015.
90. Uddin MS, Rahman MM, Jakaria M, Rahman MS, Hossain MS, Islam A, Ahmed M, Mathew B, Omar UM, Barreto GE and Ashraf GM: Estrogen signaling in Alzheimer's disease: Molecular Insights and therapeutic targets for Alzheimer's dementia. *Mol Neurobiol* 57: 2654-2670, 2020.
91. Dubal DB, Zhu H, Yu J, Rau SW, Shughrue PJ, Merchenthaler I, Kindy MS and Wise PM: Estrogen receptor alpha, not beta, is a critical link in estradiol-mediated protection against brain injury. *Proc Natl Acad Sci USA* 98: 1952-1957, 2001.
92. Li B, Lima MRM, Nie Y, Xu L, Liu X, Yuan H, Chen C, Dias AC and Zhang X: HPLC-DAD fingerprints combined with multivariate analysis of epimedii folium from major producing areas in eastern Asia: Effect of geographical origin and species. *Front Pharmacol* 12: 761551, 2021.
93. Lee D, Jeong HC, Kim SY, Chung JY, Cho SH, Kim KA, Cho JH, Ko BS, Cha IJ, Chung CG, *et al.*: A comparison study of pathological features and drug efficacy between *Drosophila* models of C9orf72 ALS/FTD. *Mol Cells* 47: 100005, 2024.



Copyright © 2025 Cong *et al.* This work is licensed under a Creative Commons Attribution 4.0 International (CC BY-NC 4.0) License